OFFICE OF NAVAL RESEARCH

Contract N00014-83-K-0470-P00003

R&T Code NR 33359-718

Technical Report No. 95

In-situ Vibrational Spectroelectrochemistry

by

S. Pons

Prepared for publication in J. Electron. Spectros. Rel. Phenomen.

Department of Chemistry
University of Utah
Salt Lake City, UT 84112

July 15, 1988

SECURITY CLASSIFICATION OF THIS PAGE

REPORT DOCUMENTATION PAGE

1a. REPORT SECURITY CLASSIFICATION: Unclassified	1b. RESTRICTIVE MARKINGS:
2a. SECURITY CLASSIFICATION AUTHORITY:	3. DISTRIBUTION / AVAILABILITY OF REPORT: Approved for public release and sale. Distribution unlimited.
2b. DECLASSIFICATION / DOWNGRADING SCHEDULE:	
4. PERFORMING ORGANIZATION REPORT NUMBER(S): ONR Technical Report No. 95	5. MONITORING ORGANIZATION REPORT NUMBER(S):
6a. NAME OF PERFORMING ORGANIZATION: University of Utah; 6b. OFFICE SYMBOL (If applicable):	7a. NAME OF MONITORING ORGANIZATION:
6c. ADDRESS (City, State, and ZIP Code): Department of Chemistry, Henry Eyring Building, Salt Lake City, UT 84112	7b. ADDRESS (City, State, and ZIP Code):
8a. NAME OF FUNDING / SPONSORING ORGANIZATION: Office of Naval Research; 8b. OFFICE SYMBOL (If applicable):	9. PROCUREMENT INSTRUMENT IDENTIFICATION NUMBER: N00014-83-K-0470-P00003
8c. ADDRESS (City, State, and ZIP Code): Chemistry Program, Code 1113, 800 N. Quincy Street, Arlington, VA 22217	10. SOURCE OF FUNDING NUMBERS: PROGRAM ELEMENT NO. / PROJECT NO. / TASK NO. / WORK UNIT ACCESSION NO

11. TITLE (Include Security Classification): In-situ Vibrational Spectroelectrochemistry

12. PERSONAL AUTHOR(S): S. Pons

13a. TYPE OF REPORT	13b. TIME COVERED	14. DATE OF REPORT (Year, Month, Day)	15. PAGE COUNT
Technical	FROM 9/87 TO 7/88	July 15, 1988	24

16. SUPPLEMENTARY NOTATION

17 COSATI CODES			18. SUBJECT TERMS (Continue on reverse if necessary and identify by block number)
FIELD	GROUP	SUB-GROUP	infrared spectroelectrochemistry

19. ABSTRACT (Continue on reverse if necessary and identify by block number)

Attached.

20. DISTRIBUTION / AVAILABILITY OF ABSTRACT: ☒ UNCLASSIFIED/UNLIMITED ☐ SAME AS RPT ☐ DTIC USERS	21. ABSTRACT SECURITY CLASSIFICATION: Unclassified
22a. NAME OF RESPONSIBLE INDIVIDUAL: Stanley Pons	22b. TELEPHONE (Include Area Code): (801)581-4760; 22c. OFFICE SYMBOL:

DD FORM 1473, 84 MAR — 83 APR edition may be used until exhausted. All other editions are obsolete.

SECURITY CLASSIFICATION OF THIS PAGE

SUMMARY

The use of infrared and Raman spectroscopies for the investigation of the electrode-solution interface is described. Applications for the studies of adsorbates, surface reactions, electron transfer reactions, and recently developed models that treat the potential dependency of vibrational bands of adsorbed species are discussed.

IN SITU VIBRATIONAL SPECTROELECTROCHEMISTRY

Stanley Pons
Department of Chemistry, University of Utah, Salt Lake City, Utah 84112 (USA)

SUMMARY

The use of infrared and Raman spectroscopies for the investigation of the electrode-solution interface is described. Applications for the studies of adsorbates, surface reactions, electron transfer reactions, and recently developed models that treat the potential dependency of vibrational bands of adsorbed species are discussed.

INTRODUCTION

In situ methods for the investigation of the electrode solution interface have been used primarily for understanding the nature of the species in the solution phase and adsorbed at the electrode surface, and their reactions. Besides being sensitive to strongly bound species, weakly bound adsorbates and solution soluble components of the reactions may be conveniently monitored. We seek, with vibrational spectroelectrochemistry, the identification of these species, their energetics, and reaction pathways and kinetics; an important advantage of these methods is the ability to monitor the temporal behavior of particular vibrational band intensity. The techniques are limited to the investigation of local phenomena; these include the interactions of electrochemically produced species with the metal surface, with other species in the solution phase, and with electrical fields and species in the electrical double layer.

The first attempts to obtain vibrational spectra of species involved in electrochemical reactions were based on infrared transmission or internal reflectance experiments through optically transparent electrodes (1-3). These electrodes consisted of thin attenuated total reflection germanium plates or thin metal films deposited on a transparent substrate, or wire mesh electrodes sandwiched between optically transparent windows. These experiments suffered from low sensitivity and a restricted number of suitably conductive and infrared transmitting electrode materials. The first attempts to observe Raman scattering from electrodes led to the discovery of surface enhanced Raman spectroscopy (SERS) (4-5). The technique involved the use of external specular reflection from bulk metal mirror electrodes, which eventually proved to be the best technique for *in situ* infrared spectroscopy. The early infrared experiments made use of a dispersive instrument and involved modulation of the electrode potential and demodulation of the reflectance signal using phase

sensitive detection (6), a technique still in wide use. The potential modulation technique was subsequently adapted to Fourier transform infrared instruments (7). These two techniques have usually been termed electrochemically modulated infrared spectroscopy (EMIRS), and subtractively normalized interfacial Fourier transform infrared spectroscopy (SNIFTIRS), respectively. Infrared reflection absorption spectroscopy (IRRAS) is an infrared reflection technique based on detection of adsorbates on any type of surface by polarization modulation; it is also commonly used in electrochemistry. (Reviews on each of these techniques have been published (8-11)).

The techniques are for the most part based on obtaining a ratio of vibrational spectra obtained at two different electrode potentials; the normalized reflectivity change is usually termed $\Delta R/R$. The resulting spectra are bipolar in nature. In these spectra, bands extending to positive values of $\Delta R/R$ are due to species at the base potential ("reactants" or initial state of the electrochemical reaction), while negative bands denote species formed when the potential is stepped to a new value (the "products" or final state of the electrochemical reaction). In polarization modulation experiments, since adsorbed species will not be detected for the tangential polarization component, the spectra are single sided (vide infra).

Infrared (EMIRS, SNIFTIRS) techniques are sensitive from about 10^{-2} down to 10^{-6} $\Delta R/R$. The frequency range presently attainable is from the near infrared down to about $80cm^{-1}$ (with Fourier transform machines). Absolute intensity measurements are possible, but difficult. Any electrode material may be used in the experiments. The cell design presently is restricted to thin layer types containing an infrared transparent window.

Raman experiments are based on single photon counting techniques; the state of the art is rapidly becoming more sophisticated (vide infra). SERS, and the newer techniques DSERS and SUERS (diminished and surface unenhanced SERS, respectively (12)) have different experimental characteristics than the infrared techniques. The SERS spectra are single sided, while due to the differential method employed for measurement, the SUERS experiments yield bipolar spectra. DSERS may have either type. Single photon counting SERS and DSERS techniques can presently be carried out from the near infrared to about $2cm^{-1}$, while SUERS has only been performed down to $200cm^{-1}$. Only relative intensities may conveniently be measured by these techniques. Until recently the electrode materials were restricted to the coinage metals for SERS and DSERS; however it has been shown that it is possible to obtain enhanced Raman signals from virtually any metal (vide infra). Electrode materials for SUERS are unrestricted. The cell design is much more versatile since infrared radiation is not employed.

IONIC ADSORPTION

The simplest systems that have been studied using SERS have been those of adsorbed halide and pseudohalide ions (13-18). There are bands observed at very low frequencies (17,19-22) which have been attributed to the interaction of the adsorbate with phonons in the SERS roughened surface. Bands are observed that have been attributed to water adsorption (17). The positions of these bands at a given potential depend strictly upon the nature of the cation present in the solution. The vibrational bands of the ions themselves are quite sharp and depend on the nature of the anion. It has been shown that the intensities of the bands are related to the surface coverage (13,18). Most interpretations have been given in terms of progressive and cation dependent desolvation at high negative potentials. Very sharp bands have been observed in the water bending region (17) indicating long range structure. These observations have now been confirmed by <u>in situ</u> X-ray diffraction techniques. As we will see below ion pairing effects must also be included in interpretations for these systems. Cyanide ion adsorption has been extensively studied (23-29). Most all results indicate that there are at least two cyanide ions adsorbed at each active site on the electrode. Water interaction is obvious; both the cyanide and hydroxyl vibrational frequencies are potential dependent. Solvent clustering is indicated from the nature of the OH bending modes. Most models attempt to explain these observations by back-bonding to the π^* orbitals on the cyanide ions from the d-orbitals in the metal surface. Orientation changes are evident in some cases; for instance, in that of $Ag(CN)_2^-$ where there is a change in orientation from C_{2v} to $D_{\infty h}$. This is a good example of the use of SERS for following reaction paths of an electrochemical reaction. In some of our very early work we were able to follow adsorption of organic electrolytes in acetonitrile solutions. Again, the dependence of water and ion pairing effects on double layer structure was quite evident. SERS has also been used extensively in the study of outer sphere redox reactions; most notably, cyanide salts of iron and ruthenium. The spectra invariably are sensitive to the nature of the associated cation and potential; in all cases, the electrochemical reactions are found to take place by adsorbed intermediates (30,31). In most cases, the solution counterions play an important part in the vibrational behavior of the adsorbed species. I will present a complete analysis of one of these systems below.

ADSORPTION OF NEUTRAL MOLECULES

SERS is also widely used for the investigation of the adsorption of neutral species with and without coadsorption of ions. Pyridine has been the most widely studied system and has been studied at many different electrodes and crystal faces (32,33). While the interpretation of the spectra have been

controversial, it is encouraging to note that the results from SERS, DSERS and SUERS are virtually identical. SERS results therefore represent the surface; the enhancement mechanism may be unimportant in the interpretation of the spectra obtained.

There has been a considerable amount of work on CO adsorbed on Pd, Pt, and Rh (36-38). In addition, studies have been carried out for the oxidation of small organic fuels where it is known that carbon monoxide is an adsorbed intermediate (39,40). IRRAS has been a popular tool in these studies. The coverage of CO on platinum for instance may be accurately controlled by changing the potential. It is interesting that there is an apparent phase transition at a surface coverage of 0.41 which is the same as that observed for the adsorption of CO from the gas phase onto palladium (41). In the gas phase, there must be only weak interaction with the solution, whereas adsorption onto the electrode in the electrochemical system requires first the desorption of specifically adsorbed bisulfate ions and water molecules. It is interesting that the transition apparently is sharper in the electrochemical system. Another important feature in spectroelectrochemical experiments is that it is possible to monitor the effect on the spectra of changes in electrode potential at constant coverage as well as changes of coverage at constant electrode potential (37,42,43). Measurements on systems with mixtures of CO isotopes have led to the conclusion that interactions between adsorbed molecules must be primarily through dipole-dipole coupling.

We and others have studied a variety of more complex adsorbates that may be adsorbed in more than one orientation on the surface. These have included several nitriles which are excellent candidates for spectroelectrochemical experiments due to the strong vibrational intensity of the cyanide moiety (37,42,46). Analysis on polycrystalline gold electrodes of the low frequency modes of adsorbed acrylonitrile (which have an abnormally low intensity) indicates that the molecule is orientated with its molecular plane parallel to the electrode. Interaction with the surface is then through the π orbitals. The difference spectra are unipolar and then must be entirely due to modulation of the band intensity by the electrochemically applied potential. The weak spectra observed are due either to the electrochemical Stark effect or to the vibronic coupling mechanism mentioned above due to partial charge transfer. The transfer is from the electrode to the π^* orbitals since the intensities decrease at higher positive potentials. We compare these results to the cyanide stretching frequency of adsorbed benzonitrile which is shifted to higher frequencies. This is common when bonding to the surface is through the nitrogen atom. In these experiments one also observes bipolar spectra due to the disappearance of species from the solution as the adsorbate is formed (the bands for these two species are at different frequencies). We have also

observed the ring modes of benzonitrile which are allowed by the surface selection rule. These modes would be forbidden if the molecule were orientated flat on the surface. A complete analysis of the adsorbed p-difluorobenzenes was also made which indicated that at some potentials and concentrations the molecules reoriented on the surface from flat configurations (low potentials, low concentrations) to edge-on configurations (high potentials, high concentrations). Temperature dependencies were also observed.

UNDERPOTENTIAL DEPOSITION

We have recently studied the low frequency vibrations for layers of lithium on gold electrodes (45,46). In these cases, we can observe the lithium-gold and the lithium-lithium vibrations directly. The most extensive work on sub-monolayer amounts of metal on SERS spectra of adsorbates on silver electrodes have been carried out by others (47-54). There are wide differences in interpretations. Some have reported (49,51) that monolayer lead tends to decrease the SERS spectra of adsorbed pyridine and chloride. In other results very small coverage of thallium also leads to decreases in the SERS intensity of the same system. However, thallium on silver only affects the SERS intensity of benzotriazole (48) slightly. Removal of deposits do not necessarily lead to regeneration of SERS; it is generally felt that the decrease in intensity is then due to the removal of adatom or adatom clusters on the surface of the SERS active electrode. The stability of the SERS surface to underpotential deposition is therefore critical to meaningful modelling of SERS quenching. Fleischmann et al. (55-57) have therefore developed new constructions for SERS. They have shown that it is possible to bury the SERS surface beneath electrodeposits and that the resulting electrode will give enhanced spectra from the interface between the electrodeposited material and the solution. Cyanide adsorption is observed on silver surfaces at potentials positive of underpotential deposition of zinc, while during underpotential deposition of zinc, cyanide adsorption onto both silver and zinc is evident. When a full layer of zinc has been deposited, only cyanide adsorbed onto zinc is detected. Zinc normally is a SERS inactive surface. The SERS signal decreases with bulk deposition of zinc; the signal for adsorbed cyanide is present until the equivalent of about 15 monolayers of zinc has been deposited. It is clear that it is possible to generate in situ a variety of metal surfaces that exhibit SERS spectra or enhanced Raman spectra. The electromagnetic fields generated in the rough silver SERS active surface can penetrate through overlayers to reach adsorbates. Finally, the SERS mechanism is stabilized by the deposition process since the silver surface is not susceptible to reorganization once it has been covered by the adlayers.

THEORETICAL CONSIDERATIONS

Introduction

A unique characteristic of the spectra of species adsorbed on electrodes is the potential dependence of the frequency of certain vibrational modes. Two types of mechanisms have been proposed to explain the potential dependent shift of band position; one explanation involves molecular orbital type arguments and the other involves an interaction between the electric field across the double layer and the highly polarizable electrons of the adsorbed molecule (an electrochemical Stark effect). In the molecular orbital mechanism, electrons can be donated to empty metal orbitals through σ-type overlap with filled ligand orbitals of the appropriate symmetry. The metal can "back" donate electrons from filled d-orbitals to empty π^* antibonding orbitals on the adsorbate. When a molecule is adsorbed on a clean uncharged metal surface, its vibrational frequency may either increase or decrease from the frequency of the unadsorbed molecule depending upon the relative contributions of the σ- and π-bonding interactions. If the π-bonding interaction is dominant the frequency will decrease; conversely, the frequency will increase if the σ-bonding interaction is dominant. When the charge on the electrode is made negative, the bond is weakened due to donation of charge from the metal into adsorbate π^* orbitals and the band frequency shifts to lower wavenumber. When the charge on the metal is made positive a shift to higher frequency occurs.

The electric field mechanism involves coupling of the electric field across the double layer with highly polarizable electrons of the adsorbate. According to the Gouy-Chapman-Stern model (58), for a large concentration of electrolyte (1.0M) most of the potential drop will occur within the first 5-10Å of the electrode surface, and this potential drop will be approximately linear with distance. When a layer of adsorbed species is present, it can act as a dielectric across which the greatest portion of the potential drop will occur. Electric fields on the order of 10^9 V m^{-1} are expected to exist in this region. Interaction of this electric field with the dipole moment of the molecule leads to changes in the vibrational frequency of the molecule. Extensive calculations have been carried out to test each of these models for adsorbed CO both in gas phase and in electrochemical systems. Some of these will be discussed below (*vide infra*).

Secondly, the intensity of certain infrared active modes of adsorbed species may be enhanced by changing the electric field across the double layer. In addition, the activation of infrared inactive (Raman active) bands in highly polarizable adsorbed species has been observed. These types of electric field effects dominate the spectra of adsorbed species with large changes in the polarizability with bond distance ($d\alpha/dr$).

The adsorption of carbon monoxide on platinum surfaces has been

extensively studied by infrared spectroscopy both in the gas phase on Pt(111) surfaces (59,60) and in aqueous solution at the surface of polycrystalline platinum electrodes (61-64). In ultra high vacuum (UHV) experiments, at least two bands have been reported in the vibrational spectrum. At low coverage there is an absorption band at 2065cm^{-1} which shifts to higher wavenumber as the coverage is increased. At intermediate and higher coverage, an additional band appears at 1850cm^{-1}. The 2065cm^{-1} band has been assigned to the C-O stretch fundamental of CO linearly adsorbed at a top site. In this model, the carbon atom is bound to the metal atom. The 1850cm^{-1} band has been assigned to CO adsorbed in a bridging site bonded to two platinum atoms. In these experiments, an absorption band is observed at 2060cm^{-1} which shifts to higher energy as the potential is made more positive; this frequency corresponds to the linearly adsorbed species. At saturation coverage, the magnitude of the potential dependent shift is linear and has a gradient of 30cm^{-1} V^{-1}.

There have been several models proposed for the potential dependent frequency shift. One model (64) suggests that CO is adsorbed as islands on the platinum surface and that oxidation to CO_2 occurs at the edges of these islands. Others have suggested that donation of electrons from filled platinum d-orbitals to empty $2\pi^*$ orbitals on the CO molecule weakens the CO bond. Electrons can be donated to the metal from the CO molecule through overlap of the filled 5σ orbital on CO with a metal σ-orbital. Ray and Anderson have modelled the adsorption of CO onto platinum clusters using an extended Huckel type method (65). The increase in positive electrode potential was simulated by increasing the valence state ionization potential on the platinum atoms. The authors find that as the ionization potential is increased the energy of the platinum s-d valence band shifts to higher energy. They suggest that this leads to less mixing of metal orbitals with the antibonding π^* orbital on CO which then affects the occupancy of the antibonding CO orbital. The CO vibrational frequency shifts to higher wavenumber as a result of the decreased antibonding character. Holloway and Norskov (66) have suggested that the electric field in the double layer shifts the energy of the $2\pi^*$ orbital thus affecting its occupancy. The occupancy of this orbital was calculated as a function of the potential (estimated from experiment) and a 30cm^{-1} V^{-1} shift in CO stretching frequency was reported.

Lambert has suggested that the shift in wavenumber is due to an interaction of the electric field across the double layer with the highly polarizable electrons of the adsorbed CO molecule. When CO is adsorbed from the gas phase on Ni(110), the dipole moment function, which is proportional to the integrated band intensity, is increased by about a factor of two. Lambert calculates a Stark tuning rate of 9.0 x 10^{-9}cm^{-1} V m^{-1} for this system (67) Using this tuning rate and by estimating the change in field with applied

potential for the electrochemical system he is able to reproduce the $30cm^{-1}$ V^{-1} shift in band position. Thus, for high fields which exist across the double layer (on the order of $10^9 V\ m^{-1}$) the molecule is easily perturbed.

Species involved in electrochemical processes are influenced by the surrounding environment. Interactions of electroactive species with solvent, electrolyte, and electrode materials are manifested in the infrared spectrum of the species. Methods for evaluating the effects these perturbations have on vibrational spectra have been difficult to develop. Conventional normal coordinate analysis involves defining a set of force constants in terms of the internal coordinates of the molecule. The complete potential is described in terms of the sum of the harmonic force constants for the molecule. The internal coordinate force constant matrix can be transformed to normal coordinate force constants and determination of the normal mode vibrational frequencies follows directly. Although this method is quite popular and is extremely useful for the vibrational analysis of molecules which are largely undisturbed by the environment, it is not well suited for the analysis of the spectra of molecules under the effects of external perturbations, such as those present on an adsorbate; there is no general or simple way to introduce the external forces into the internal coordinates. It is simpler to develop an analysis based on direct interaction of the atomic centers.

We have developed a simple model for this purpose (68). In this method, cartesian force constants are obtained for the displacement of atoms from their equilibrium positions. A potential energy function is developed for the system as the sum of pair-wise potentials operating between the bonded and nonbonded atoms in the molecule. Perturbations are easily introduced by additional pair-wise terms operating between the perturbing species and the specific atoms in the molecule. The force constants can be derived for the system by expansion of the individual potential energy functions to second order in a Taylor series. The cartesian force constant matrix is transformed to the normal coordinate force constant matrix and the normal mode vibrational frequencies are obtained directly.

Application to adsorbed carbon monoxide

We have applied this method to the analysis of the potential dependent frequency shift of carbon monoxide adsorbed on platinum electrodes (68). This analysis has been carried out in particular for CO adsorbed on Pt(111) surfaces since the behavior is similar to CO adsorbed on platinum electrodes.

The potential energy is developed as the sum of pair-wise interactions for the various atoms in the system. Specifically:

$$V = V_{CO} + V_{CS} + V_{OS}. \qquad (1)$$

In this expression, V_{CO} is a Morse potential which represents the underlying bonding in carbon monoxide,

$$V_{CO} = D \exp[a(r^0_{co} - r_{co})]\{\exp[a(r^0_{co} - r_{co})] - 2\}. \quad [2]$$

The values of D, a, and r^0_{co} are those for an isolated carbon monoxide molecule; r_{co} is the carbon-oxygen separation. The function V_{CS} describes the interaction of carbon with the surface. A Lennard-Jones potential was used for the interaction of the carbon atom with each of the surface atoms, so V_{CS} is

$$V_{CS} = \epsilon \sum_i (c/r_{ci})^6[(c/r_{ci})^6 - 2] \quad [3]$$

in which the radii r_{ci} are the distances between the carbon atom and each platinum atom i. The model of the platinum surface consists of 14 platinum atoms arranged in a (111) configuration. The last term in the potential, V_{OS}, represents the oxygen-surface interaction. We used a sum of Morse potentials for each of the oxygen atom-surface atom interactions,

$$V_{OS} = \sum_i D'\exp[\gamma(r^0_{oi} - r_{oi})]\{\exp[\gamma(r^0_{oi} - r_{oi})] - 2\} \quad [4]$$

in which the r_{oi} are the distances between the oxygen and each platinum atom.

The parameters in the expression for the interaction potential are listed in (70). The parameters in V_{CO} were arbitrarily chosen to be those for gas-phase carbon monoxide. The parameter r^0_{oi} in V_{OS} was chosen to make this a repulsive term; the remaining parameters in V_{CS} and V_{OS} were optimized by a least squares fit to the experimental binding energies and the carbon-oxygen and platinum-carbon vibrational frequencies as found under uhv conditions for carbon monoxide bonded both to on-top and bridging sites. Complete C-O and Pt-C bond length optimizations were performed at each site by the Newton-Raphson method. The geometry was optimized with carbon monoxide bound normal to the surface, with the carbon end towards the metal. The binding energy was calculated as the difference between the total energy and the dissociation energy of isolated carbon monoxide. The parameters in the V_{CS} and V_{OS} parts of the potential were refined until the calculated binding energy and vibrational frequencies gave acceptable agreement with experiment.

Assuming that the binding energies of the surface/adsorbate interactions vary with potential, it has been shown that for linear changes in the binding energies (D' and ϵ) the CO vibrational frequency shifts linearly. An electric field type perturbation has also been applied to the system by adding the new quantity V_{field} to the interaction potential:

$$V_{field} = E_z M(z^0 - z) \qquad [5]$$

The purpose of the perturbation was to see if a Stark effect could be seen. A potential of this type is consistent with the Gouy-Chapman-Stern theory of the electrical double layer (58). In this expression E_z is the electric field strength in a direction normal to the surface, M is (du/dz) obtained from expansion of the dipole moment function, and the term (z^0-z) is the relative displacement of the atom from its equilibrium position (z^0) in a direction normal to the surface. The experimental value of (du/dz) for CO in gas phase is 3.093D $Å^{-1}$ (69). Lambert has found that this value increases by about a factor of 2 when CO is adsorbed on Ni(110) (67). Therefore, to calculate the electric field perturbation (du/dz) was taken to be 6.18D $Å^{-1}$. Using this model, a Stark tuning rate of 9.0 x 10^9 cm^{-1} V m^{-1} was calculated which is in excellent agreement with Lambert's result (67).

Application to adsorbed hexacyanoferrate

We have applied this model to the analysis of the vibrational frequencies of ferricyanide and ferrocyanide adsorbed on metal electrodes (70). In homogeneous solution rate of electron transfer depends upon the nature and concentration of cations in solution. In heterogeneous electron transfer reactions, the rate depends upon electrode material as well as the nature and concentration of cations in solution (72-76). In both cases mechanisms apparently involve the association of a solution cation with the complex ion.

Several models of the have been suggested to explain the kinetic behavior at the electrode surface. Schleinitz et. al. (74,75) proposed formation of a dimeric species in which a cation bridge is formed between the reacting species. Sohr et. al. have proposed a similar species and have suggested stabilization by the surface (77). Radiotracer and voltammetric studies of the redox couple indicates adsorption of $[Fe(CN)_6]^{3-}$ onto platinum electrodes; the interaction apparently involves one or two cyanide ligands bonded to the surface through a nitrogen atom (78). Other workers have presented ion-pairing arguments to explain the differences in reaction rates under the different solution environments. Peter et. al. studied the kinetics of the reaction at a gold electrode in the presence of various cations (77). The electron transfer rate was found to increase with the concentration of the cation and in the order $Li^+ < Na^+ < K^+ < Cs^+$. They suggested formation of an activated complex in which at least two cations are associated with the hexacyanoferrate. In situ vibrational spectroscopic methods have been used to investigate this system (79-81). These studies also indicate adsorption of ferricyanide and ferrocyanide species and show that changes occur in the structure of the complex when the solution cation is changed. The ferricyanide/ferrocyanide

electron transfer reaction has been studied at platinum, gold, and β-palladium hydride electrodes. The $[Fe(CN)_6]^{4-}$ / $[Fe(CN)_6]^{3-}$ couple at platinum electrodes has strong bands at 2040 cm^{-1} and 2114 cm^{-1} which correspond to F_{1u} modes of solution soluble ferrocyanide and ferricyanide respectively. There is a strong and potential dependent band at 2092 cm^{-1} and a weaker shoulder at about 2061 cm^{-1} for the oxidation of $[Fe(CN)_6]^{4-}$; they are not present in the spectrum corresponding to $[Fe(CN)_6]^{3-}$ reduction. The 2092 cm^{-1} band is due to an adsorbed iron species and the 2061 cm^{-1} band is adsorbed CN^- formed as a result of the catalytic surface decomposition of $[Fe(CN)_6]^{3-}$ (79).

SERS spectra of the ferricyanide/ferrocyanide couple were obtained at gold electrodes. The spectra were measured as a function of electrode potential and type of alkali metal cations (80-81). The SERS data provide more evidence for adsorption of both $[Fe(CN)_6]^{4-}$ and $[Fe(CN)_6]^{3-}$ species at the surface. The spectra show absorbances in the 2050 cm^{-1} to 2200 cm^{-1} range. These were assigned to C=N stretching A_{1g} and E_g modes. These spectra depend upon both the nature of the cation and the applied electrode potential. In every experiment, the bands are shifted to higher frequencies compared to the solution soluble hexacyanoferrate. The shifts were attributed to electron withdrawing effects from interaction with the cations in solution and with the electrode surface. A summary of the spectral features is given in Table 1.

Table 1
Summary of spectral band positions from SERS spectra (80).
Potential is in Volts vs. SCE, and band positions are in cm^{-1}.

	Vibrational bands (cm^{-1})				
Cation	$[Fe(CN)_6]^{3-}$		$[Fe(CN)_6]^{4-}$		
E/V	+0.4	+0.3	+0.2	+0.1	0.0
Li^+	2189	2184	2129	2128	2100
		2129	2103	2104	
		2103			
Na^+	2186	2147	2150	----	2156
	2150				2090
K^+	2150	2150	2150	----	2125
Cs^+	2130	2130	2130	2130	2127
	2093	2090	2087	2087	2087

A potential energy function to describe the interactions of ferricyanide and ferrocyanide with a metal electrode was constructed as follows. The complete form of the potential is given by

$$V = V_F + V_S + V_{IP} \qquad [6]$$

The term V_F is the potential of the unperturbed ferricyanide or ferrocyanide molecule. This interaction was derived from a modified Urey-Bradley force field (MUBFF) from Nakagawa and Shimanouchi (82). The potential V_F contains two contributions: $V_{pair\text{-}wise}$ in which the harmonic bond stretching (K_1 and K_2) and non-bonded interaction (F) terms of the original MUBFF were fitted to Morse or Lennard-Jones functions, and V_{UBFF} which contains the angle bending (H_1 and H_2) and bond interaction (p_1 and p_2) terms of the original MUBFF. Specifically,

$$\begin{aligned} V_{pair\text{-}wise} = {} & D_1 \Sigma_i \exp[\gamma(r^0_{FeC} - r_{FeC(i)})]\{\exp[\gamma(r^0_{FeC} - r_{FeC(i)})] - 2\} \\ & + D_2 \Sigma_i \exp[\gamma'(r^0_{CN} - r_{CN(i)})]\{\exp[\gamma'(r^0_{CN} - r_{CN(i)})] - 2\} \\ & + \epsilon \Sigma_{i,j} (r^0_{CC}/r_{CC(i,j)})^6[(r^0_{CC}/r_{CC(i,j)})^6 - 2] \end{aligned} \quad [7]$$

$$\begin{aligned} V_{UBFF} = {} & (H_1 \Sigma_{j,k} (r^0_{FeC})^2(\Delta\alpha_{j,k})^2 + (H_2 \Sigma_{j,k} (r0_{FeC})(r0_{CN})(\Delta\beta_{j,k})^2 \\ & + p_1 \Sigma_{j,k} (\Delta r_{FeC})(\Delta r_{CN}) + p_2 \Sigma_{i} (\Delta r_{FeC})(\Delta r'_{FeC}). \end{aligned} \quad [8]$$

In these expressions r^0_{FeC}, r^0_{CN}, and r^0_{CC} are the equilibrium bond distances and D_1, D_2, and ϵ represent the bond dissociation energies for the bonded Fe-C, C≡N, and adjacent non-bonded carbon interactions. The $r_{FeC(i)}$ and $r_{CN(i)}$ represent the ith Fe-C and C≡N bond distances. The $r_{CC(i,j)}$ represent the distance between the ith and jth non-bonded adjacent carbon atoms. The terms γ and γ' are the usual Morse parameters. The terms in V_{UBFF} are identical with the angular and interaction terms used in the modified Urey-Bradley potential of Nakagawa and Shimanouchi. The $\alpha_{i,j}$ and $\beta_{i,j}$ are the C-Fe-C and the Fe-C≡N bond angles, and the H_1 and H_2 are the C-Fe-C and Fe-C≡N angle bending force constants. The p_1 terms are the interaction force constants between two Fe-C bonds on the same diagonal and the p_2 terms are the interaction force constants between adjacent Fe-C and C≡N bonds.

The numerical values used for these potentials are given in (70); and Table 2 lists the vibrational frequencies calculated from the potential V_F.

Table 2
Summary of calculated and observed C≡N frequencies in cm^{-1}.

Species	Mode	C≡N Vibrational bands (cm^{-1})					
		$[Fe(CN)_6]^{3-}$			$[Fe(CN)_6]^{4-}$		
		Obs.(82)	Calc.(82)	Calc.	Obs.(82)	Calc.(82)	Calc
A_{1g}	ν_1	2136	2123	2123	2080	2017	2017
E_g	ν_3	2136	2115	2115	2048	2010	2010
F_{1u}	ν_6	2105	2124	2124	2021	2020	2020

The experimentally observed values and those calculated by Nakagawa and Shimanouchi are compared in the table. The bond distances used for the ions in solution were 2.0Å for the Fe-C bond, and 1.15Å for the C-N bond. The Morse parameters γ and γ' were chosen to be $2.0Å^{-1}$, and the dissociation energies D_1, D_2, and ϵ were determined from the harmonic st·etching force constants. The term V_S is

$$V_S = D_3 \sum_m \exp[\rho(r^0_{SN} - r_{SN(m)})][\exp[\rho(r^0_{SN} - r_{SN(m)})] - 2) \quad [9]$$

and is the interaction between the metal surface and the hexacyanoferrate molecule. The parameter D_3 is the molecule-surface dissociation energy. The ferri- and ferrocyanide surface binding energies are unknown; we know however that adsorbate-metal binding energies on the order of 1 eV are quite common. In each case, therefore, a range of values for D_3 was tried until the adsorbate-surface binding energy was between 0.1 eV and 1.0 eV. The term r^0_{SN} is the equilibrium nitrogen-surface bond distance for the two-center term, and was chosen to limit the long range surface attraction to prevent large perturbations of the nitrogen atoms directed away from the surface. The term $r_{SN(m)}$ is the actual nitrogen-surface distance. As the atomic level structure of the electrode surface is unknown, we modeled the surface perturbation as an effective pair potential rather than as specific atom-atom interactions (83).

V_{IP} is the ion-pairing interaction between the ferro/ferricyanide anion and alkali metal cations:

$$V_{IP} = (D_4 / 11) \Sigma_{i,j} [(r^0_{IN}/r_{IN(i,j)})^{12} - 12(r^0_{IN}/r_{IN(i,j)})] \quad [10]$$

where r^0_{IN} is the equilibrium ion-nitrogen distance calculated from the van der Waals radii of the ions, and $r_{IN(i,j)}$ is the distance between the ith ion and jth nitrogen atom. The ion-nitrogen dissociation energy is given by D_4 and was determined from the heat of formation of the ions in an aqueous solution (84). The values for all of the terms are listed in (70).

In all cases, the geometry of the system was optimized using the Newton-Raphson method. The Cartesian force constants for the angle-bending and stretch-stretch interaction terms in V_{UBFF} were calculated using standard methods (85,86). The Fe-C≡N linear bending force constant (H_2) was set to zero for the calculation of the vibrational frequencies of the adsorbed species. We are interested in the changes in the C≡N stretching frequencies, and we found that setting H_2 to zero resulted in less than a 1 cm^{-1} change.

The analysis was made for both ferricyanide and ferrocyanide adsorbed in three basic orientations on the surface, ie. with one, two, or three cyano

groups in contact with the surface. The free energy of adsorption increases with the number of cyano groups in contact with the surface. As the surface-adsorbate potentials are only approximate, a simplified model of the surface interaction was used. The effect of applied electrode potential were simulated by changing the nitrogen-surface binding energy (D_3). We assume that some relationship between binding energy and applied electrode potential

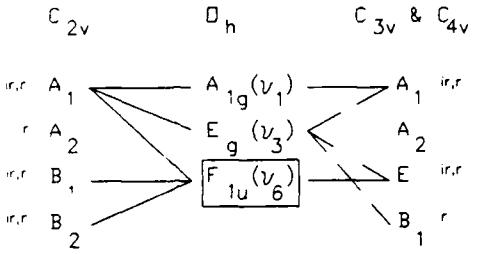

Figure 1. Splitting of the A_{1g}, E_g, and F_{1u} modes into their symmetry species in the C_{2v}, C_{3v}, and C_{4v} point groups. Splitting of the E_g mode according to C_{4v} symmetry is indicated by (----), and (-.-) for C_{3v} symmetry.

does exist. For CO adsorbed on platinum electrodes a relationship of this type has been suggested (86). It has been shown that the frequency of the CO stretching mode varies linearly with changes in binding energy (83). In bonding to the surface the symmetry of the molecule is perturbed from that of the octahedral point group. Figure 1 shows the splitting for the A_{1g}, E_g, and F_{1u} modes when the molecule is adsorbed in the three orientations shown above. Since these were the major modes observed in the spectra, they were the only modes considered in the analysis. The C_{4v}, C_{2v}, and C_{3v} symmetry species correspond to bonding to the surface through one, two, and three nitrogen atoms respectively. It should be noted that when the molecule has octahedral symmetry the X_g modes are Raman active but not infrared active. Also, the X_u modes are infrared active and have no Raman activity. However, when the symmetry of the species is perturbed by the surface interaction, these species are split to give modes which are <u>both</u> Raman and infrared active. Therefore, when the species are adsorbed on the metal surface the SERS spectra should reflect the symmetry perturbation and contain new modes not observed in the solution spectra. Of particular interest is the infrared active F_{1u} mode of solution free ferricyanide and ferrocyanide. When the species is adsorbed onto the surface this mode splits into two (for the C_{4v} or C_{3v} configurations) or three (for the C_{2v} configuration) symmetry species all of which are Raman active. When bonding is through one nitrogen atom the infrared active F_{1u} mode splits into A_1 and E symmetry species. In this configuration the frequency of the A_1 mode varies linearly with binding energy with a slope of 224 cm^{-1} eV^{-1}

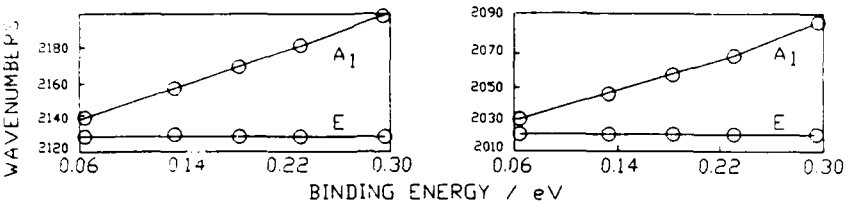

Figure 2. Splitting of the infrared active F_{1u} mode into A_1 and E symmetry species as a function of binding energy when (left) ferricyanide and (right) ferrocyanide are bonded to the surface through one nitrogen atom.

and 232 cm^{-1} eV^{-1} for the ferri- and ferrocyanide species respectively. The doubly degenerate E mode is unchanged with electrode binding energy (Figure 2). When bonding is through three nitrogen atoms in a C_{3v} configuration the dependence of the A_1 and E modes on binding energy (Figure 3) is diminished compared to the C_{4v} configuration. The A_1 and E modes of both the ferricyanide and ferrocyanide species have slopes of 26 cm^{-1} eV^{-1} and 25 cm^{-1} eV^{-1} respectively. When ferricyanide or ferrocyanide bonds through two nitrogen atoms in a C_{2v} configuration the F_{1u} mode splits into A_1, B_1, and B_2 modes. Figure 4 shows the splitting of these modes as a function of electrode binding energy. Both A_1 and B_2 modes shift linearly with 58 cm^{-1} eV^{-1} for the ferricyanide species. Shifts of 60 cm^{-1} eV^{-1} and 54 cm^{-1} eV^{-1} are observed for

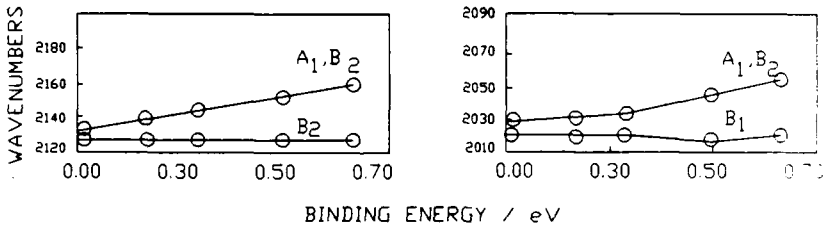

Figure 3. Splitting of the infrared active F_{1u} mode into A_1 and E symmetry species as a function of binding energy when (left) ferricyanide and (right) ferrocyanide are bonded to the surface through three nitrogen atoms.

the A_1 and B_2 modes of ferrocyanide. The frequency of the B_1 mode is unchanged with binding energy. The frequencies of the adsorbed species which arise from splitting of the A_{1g} and E_g modes vary with binding energy by only a few wavenumbers and are the same as those in Table 2 for the A_{1g} and E_g modes.

The effect of ion-pairing of hexacyanoferrate with Li^+, Na^+, K^+, and Cs^+ was simulated with the interaction term. In aqueous solution the association energy of these cations with ferricyanide and ferrocyanide is small, on the order of 2 kJ $mole^{-1}$ for the $K_3[Fe(CN)_6]$ complex and 4.2 kJ $mole^{-1}$ for the $K_4[Fe(CN)_6]$ species (84). The effects of one, and two ion pairing cations were tested with the solution free and surface bound $[Fe(CN)_6]^{4-}$ and $[Fe(CN)_6]^{3-}$ species. In each case the changes in frequency were slight, less than 0.01 cm^{-1}. The model was also tested by increasing the

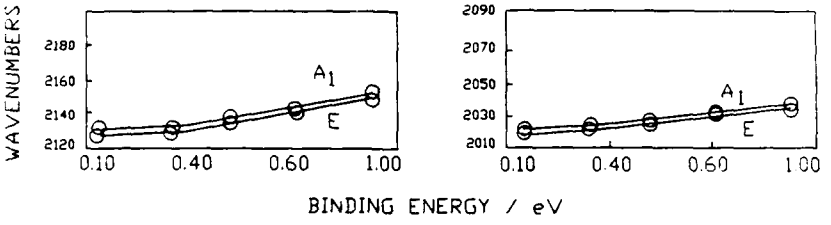

Figure 4. Splitting of the infrared active F_{1u} mode into A_1, B_1, and B_2 symmetry species as a function of binding energy when (left) ferricyanide and (right) ferrocyanide are bonded to the surface through two nitrogen atoms.

binding energy by a factor of ten for the increased ion-pairing by lithium. Similar results were obtained.

It is important to consider the effects of symmetry perturbations which occur when the ferrocyanide or ferricyanide is adsorbed on the metal surface, as splitting of the (infrared active) F_{1u} mode of the solution species is predicted to give modes which, in the new symmetry point groups of the adsorbed species, are both infrared and Raman active. According to the theoretical vibrational spectra, for binding energies as small as 0.1 eV, modes arising from splitting of the F_{1u} mode shift in energy by an amount similar to the potential dependent band in the SERS spectra. However, even for large changes in binding energy only slight shifts are observed which arise from perturbation of the A_{1g} and E_g modes of the ions in solution. The SERS spectra are characterized by a strong asymmetric band between 2190 cm^{-1} and 2130 cm^{-1} which occurs when the electrode is driven to high positive (> +0.2 V vs. SCE) potentials. The position of the band depends upon the magnitude of the electrode potential and the nature of the cation in solution. By comparison with model calculations this band can be assigned to the splitting of the degenerate F_{1u} mode upon adsorption of ferricyanide onto the electrode surface. For the C_{4v} configuration, the A_1 mode (of the A_1 and E pair) is observed at

high frequencies and has a marked potential dependence (Figure 2), a pattern of behavior which is observed typically for Li^+ containing solutions. For the C_{3v} configuration, the frequency and potential dependence is markedly reduced for both the A_1 and E modes (Figure 3), a pattern which is observed for solutions containing the Cs^+ cations. In the C_{2v} configuration, the A_1 and B_2 modes (of the three species, Figure 4) would show behavior intermediate to that for the C_{3v} and C_{4v} configurations. It is important that other Raman active vibrations, in particular those arising from splitting of the A_g and E_g modes of the octahedral solution soluble species, occur between about 2120 cm^{-1} and 2100 cm^{-1} and can be observed in the experimental spectrum as a strong shoulder extending to about 2100 cm^{-1}. The frequencies of these bands are close to those of the solution free species. The observed intensities of these modes are relatively weak presumably because of the low surface coverage by the ions in these relatively unperturbed configurations.

An additional characteristic in the SERS spectra is the effect of cations, as the intense band between 2190 cm^{-1} and 2130 cm^{-1} shifts to higher energy with increasing ion-pairing ability of the cation in solution. However, due to the weak association of the cation with the hexacyanoferrate species in aqueous solution, ion-pairing leads to shifts in the calculated vibrational frequencies of only a few wavenumbers. This discrepancy can be resolved if the strength of the ion-pair bond determines the configuration of the anion at the surface. In solution, the strongest interaction of ferricyanide and ferrocyanide is with Li^+ and such ion-paired species may well be adsorbed via a single nitrogen atom. By contrast, weak interaction with Cs^+ would allow the anions to take up the most energetically favorable C_{3v} bonding configuration. It is possible then that weak association of the electroactive species with cations stabilizes the adsorbate-surface interaction. These conclusions are supported by radiotracer studies which have shown that, in the presence of potassium ions, ferricyanide adsorption occurs via one or two nitrogen atoms (78). It is interesting to note that, compared to other alkali metal cations, the weakest spectral perturbations and the fastest electron transfer rates are observed when cesium is the alkali metal cation present in solution. If the adsorbate surface orientation is indeed influenced by ion-pairing, then the ion-pairing interaction may play a major role in determining the structure of the anion-surface interactions and thus the structure of the transition state of the heterogeneous electron transfer reaction. We have also studied this system by <u>in situ</u> infrared spectroscopy (79). It has been suggested that the potential dependent band at 2092 cm^{-1} is due to ferricyanide adsorbed with the C≡N groups oriented parallel to the surface (rather than end-on via the nitrogen atom) based on the shifting to lower energies by ferricyanide bands with potential. This interaction was simulated by application of an additional interaction

between the surface and carbon atoms of the ferricyanide. At the equilibrium geometry, the molecule was unrealistically deformed and only small spectral shifts were observed. It is possible that the deformation and small spectral shifts arise from neglect of the linear bending force constant (H_2). However, parallel bonding is inconsistent with the SERS data shifting to higher energies is observed with increase of potential. In addition, Niwa and Doblhofer have shown by ex situ infrared reflection spectroscopy that Prussian blue is formed at platinum and gold electrodes when oxidation of ferrocyanide occurs at high positive potentials (87). Prussian blue has a characteristic absorption band at 2090 cm^{-1}. Therefore, it is likely that the 2092 cm^{-1} band arises from decomposition of ferricyanide during oxidation of ferrocyanide. Within the limits of the model described above we conclude that adsorption of ferricyanide and ferrocyanide on metal electrodes is an important step in the heterogeneous electron transfer reaction. It appears that ion-pairing with alkali metal cations may stabilize particular surface-adsorbate orientations. These orientations explain the nature of the spectra of the adsorbed species observed by Raman and infrared spectroscopy and the behavior of the spectra with changes in cation and electrode potential. The simplicity of the model should be noted. Actual surface-adsorbate interactions may be much more complex; thus, this model does not account for large changes in electronic structure which must occur upon adsorption and which must be important in determining the kinetics of the ferri/ferrocyanide redox reaction; it can be used effectively to assess qualitatively the nature of the intramolecular interactions.

REFERENCES

1. H.B. Mark, S. Pons, Anal. Chem., 38, 119 (1966).
2. A.H. Reed, E. Yeager, Electrochim. Acta, 15, 1345 (1970).
3. D. Tallant, D. Evans, Anal. Chem., 41, 835 (1969).
4. M. Fleischmann, P.J. Hendra, A.J. McQuillan, J. Chem. Soc., 80 (1973).
5. M. Fleischmann, I.R. Hill, "Electrochemical Effects in Surface Enhanced Raman Scattering", R.K. Chang and T.E. Furtak Eds. Plenum New York (1982).
6. A. Bewick, abstract Electrochem. Soc. Meeting, Montreal, 1982.
7. S. Pons, A. Bewick, Naval Research Reviews, 307 (1985) 33.
8. J.K. Foley, C. Korzeniewski, J.L. Daschbach, S. Pons, Electroanalytical Chemistry", A.J. Bard, Ed.; Marcel Dekker New York, 1986; Vol. 14, Chpt.4.
9. A. Bewick, S. Pons, Advances in Infrared and Raman Spectroscopy, R.J.H. Clark, R.E. Hester, Eds.; Wiley, New York, 1985; Vol. 12, p.1.
10. S. Pons, J.K. Foley, J. Russell, M. Severson, "Modern Aspects of Electrochemistry", J. Bockris, B. Conway, Eds. Plenum, N.Y., Vol.17 1986.
11. J.K. Foley, S. Pons, Anal. Chem., 57 (1985) 945A.
12. M. Fleischmann, P. Graves, J. Robinson, J. Electroanal. Chem., 182 (1985) 73.
13. M. FLeischmann, P. Hendra, I. Hill, M. Pemble, J. Electroanal. Chem., 117 (1981) 243.
14. B. Pettinger, M. Philpott, and J. Gordon, Surf. Sci., 74 (1981) 934.
15. B. Pettinger, M. Philpott, and J. Gordon, Surf. Sci., 105 (1981) 469.
16. H. Wetzel, H. Gerischer, B. Pettinger, Chem. Phys. Lett., 78 (1981) 392.
17. M. Fleischmann and I.R. Hill, J. Electroanal. Chem., 146 (1983) 369.

18. M. J. Weaver, J.T. Hupp, F. Barz, J.G. Gordon, and M.R. Philpott, J. Electroanal. Chem., 160 (1984) 321.
19. D. Weitz, T. Gramila, A. Genack, J. Gersten, Phys. Rev. Lett., 45 (1980) 355.
20. D. Weitz, T. Gramila, A. Genack, J. Gersten, Phys. Rev. Lett. B, 22 (1980) 4562.
21. D. Weitz, T. Gramila, A. Genack, in ref. 33, p339.
22. M. Fleischmann, I.R. Hill, J. Robinson, Chem. Phys. Lett., 97 (1983) 441.
23. J. Billman, G. Kovacs, and A. Otto, Surf. Sci., 92 (1980) 153.
24 R.E. Benner, R. Dornhaus, R. Chang, B. Laube, Surf. Sci., 101 (1980) 341.
25. R. Kotz and E. Yeager, J. Electroanal. Chem., 123 (1981) 335.
26. M. Fleischmann, I. Hill, M. Pemble, J. Electroanal. Chem., 136 (1982) 361.
27. T. Billman and A. Otto, Surf. Sci., 138 (1984) 1.
28. T. Chen, K. von Raben, D. Murphy, R. Chang, B. Laube, Surf. Sci., 143 (1984) 369.
29. M. Fleischmann, G. Sundholm, Z.Q. Tian, Electrochim. Acta, 31 (1986) 907.
30. M. Fleischmann, P.R. Graves, and J. Robinson, J. Electroanal. Chem., 182 (1985) 87.
31. M. Weaver, P. Gao, D. Gosztola, M.L. Patterson, and M.A. Tadayyoni, in A.P.B. Lever (Ed), Excited States and Reactive Intermediates, ACS Symposium Series, 307 (1986) 135.
32. T.E. Furtak and R.K. Chang (Eds.), Surface Enhanced Raman Scattering, Plenum Press, New York and London, (1982).
33. H. Seki, J. Electron Spectros. Related Phenomena, 30 (1983) 287.
34. J.W. Russell, J. Overend, K. Scanlon, M. Severson, and A. Bewick, J. Phys. Chem., 86 (1982) 3066.
35. J.W. Russell, J. Overend, K. Scanlon, M. Severson, and A. Bewick, J. Phys. Chem., 87 (1983) 293.
36. B. Beden, A. Bewick, K. Kunimatsu, and C. Lamy, J. Electroanal. Chem., 142 (1982) 345.
37. A. Bewick and T. Salomun, J. Electroanal. Chem., 150 (1983) 481.
38. A. Bewick, M. Razaq, and J. Russell, personal communication.
39. B. Beden, C. Lamy, A. Bewick, K. Kunimatsu, J. Electroanal. Chem., 121 (1981) 243.
40. B. Beden, C. Lamy, and A. Bewick, J. Electroanal. Chem., 148 (1983) 147.
41. A.M. Bradshaw and R.M. Hoffmann, Surf. Sci., 72 (1978) 513.
42. A. Bewick and S. Pons, "Infrared Spectroscopy of the Electrode-Electrolyte Solution Interface", in R. J. H. Clark and R. E. Hester, eds., "Advances in Infrared and Raman Spectroscopy", 12, Heyden and Sons, Ltd., London, 1985, p.1.
43. A. Bewick, Symposium on the Chemistry and Physics of Electrocatalysis, The Electrochemical Society, 84-12 (1984) 301.
44. A. Bewick and C. Pender, personal communication.
45. J. Li., S. Pons, and J.J. Smith, Langmuir, 2 (1986) 297.
46. J. Li., J. Daschbach, J.J. Smith, M.D. Morse, and S. Pons, J. Electroanal. Chem., 209 (1986) 387.
47. B. Pettinger and L. Moerl, J. Electron. Spectros. Related Phenomena, 29 (1983) 383.
48. J.J. Kester, J. Chem. Phys., 78 (1983) 7466.
49. A.L. Guy, B. Bergami, and J.E. Pemberton, Surf. Sci., 150 (1985) 226.
50. T.E. Furtak and D. Roy, Phys. Rev. Lett., 50 (9183) 1301.
51. T. Watanabe, N. Yanagihara, K. Honda, B. Pettinger, and L. Moerl, Chem. Phys. Lett., 96 (1983) 649.
52. Y. Gao and T. Lopez-Rios, Phys. Rev. Lett., 53 (1984) 2583.
53. T. Lopez-Rios, Y. Gao, and G. Vuye, Chem. Phys. Lett., 11 (1984) 249
54. T. Lopez-Rios and Y. Gao, J. Vacuum Sci. Technol., 83 (1985) 1539.
55. M. Fleischmann, Z.Q. Tian, and L.J. Li., J. Electroanal. Chem., in press.
56. M. Fleischmann, Z.Q. Tian, J. Electroanal. Chem., in press.
57. M. Fleischmann, Z.Q. Tian, J. Electroanal. Chem., in press.
58. A. J. Bard, L. Faulkner, "Electrochemical Methods Fundamentals and Applications", John Wiley and Sons: New York, 1980.

59. H.J. Krebs, H. Luth, Appl. Phys., 14 (1977) 337.
60. M.D. Baker, M.A. Chester, in "Vibrations at Surfaces", R. Caudano, J. M. Gilles, A. A. Lucas, eds.; Plenum: New York, 1982.
61. J.W. Russell, J. Overend, K. Scanlon, M.W. Severson, A. Bewick, J. Phys. Chem., 86 (1982) 3066 ; J.W. Russell, M.W. Severson, K. Scanlon, J. Overend, A. Bewick, J. Phys. Chem., 87 (1983) 293.
62. B. Beden, A. Bewick, K. Kunimatsu, C. Lamy, J. Electroanal. Chem., 142 (1985) 345.
63. W. G. Golden, K. Kunimatsu, H. Seki, J. Phys. Chem., 88 (1984) 1274.
64. K. Kunimatsu, W. Golden, H. Seki, M. R. Philpott, Langmuir, 1 (1985) 24.
65. N.K. Ray, A.B. Anderson, J. Phys. Chem., 86 (1982) 4851 .
66. S. Holloway, J.K. Norskov, J. Electroanal. Chem. 161 (1984) 193.
67. D.K. Lambert, Solid State Commun., 51 (1984) 297.
68. C. Korzeniewski, S. Pons, P.P. Schmidt, M.W. Severson, J. Chem. Phys., 85 (1986) 4153.
69. J. Bouanich C. Brodbeck, J. Quant. Spect. Radiat. Transfer 14 (1974) 119.
70. C. Korzeniewski, S. Pons, M. Severson, P. Schmidt, J. Phys. Chem., press.
71. M. Shporer, G. Ron, A. Loewenstein, G. Navon, Inorg. Chem., 4 (1965) 361.
72. J. Kuta, E. Yeager, J. Electroanal. Chem., 59 (1975) 110.
73. P. Bindra, H. Gerischer, L.M. Peter, J.Electroanal. Chem., 57 (1974) 435.
74. K.D. Schleinitz, R. Landsberg, G.V. Lowis von Menar, J. Electroanal. Chem., 28 (1970) 279.
75. K.D. Schleinitz, R. Landsberg, G.V. Lowis von Menar, J. Electroanal. Chem., 28 (1970) 287.
76. R. Sohr, L. Muller, R. Landsberg, J. Electroanal. Chem., 52 (1974) 55.
77. R. Sohr and L. Muller, Electrochim. Acta, 20 (1975) 451.
78. A. Wieckowski and M. Szklarczyk, J. Electroanal. Chem., 142 (1982) 157.
79. S. Pons, M. Datta, J.F. McAleer, A.S. Hinman, J. Electroanal. Chem., 160 (1984) 369.
80. M. Fleischmann, P.R. Graves, J. Robinson, J. Electroanal. Chem., 182 (1985) 87.
81. M. J. Weaver, P. Gao, D. Gosztola, M. L. Patterson, M. A. Tadayyoni, in A.P.B. Lever, ed. "Excited States and Reaction Intermediates", ACS Symposium Series 307 (1986) 135.
82. I. Nakagawa and T. Shimanouchi, Spectrochimica Acta, 18 (1962) 101.
83. C. Korzeniewski, S. Pons, P.P. Schmidt, M.W. Severson, J. Chem. Phys. 85 (1986) 4153.
84. W.A. Eaton, P. George, G.I.H. Hanania, J. Phys. Chem., 71 (1967) 2016.
85. M. A. Pariseau, I. Suzuki, and J. Overend, J. Chem. Phys. 42 (1965) 2335.
86. S. Holloway and J.K. Norskov, J. Electroanal. Chem., 161 (1984) 193.
87. K. Niwa and K. Doblhofer, Electrochimica Acta, 31 (1986) 439.

DL/1113/87/2

TECHNICAL REPORT DISTRIBUTION LIST, GEN

	No. Copies
Office of Naval Research Attn: Code 1113 800 N. Quincy Street Arlington, Virginia 22217-5000	2
Dr. Bernard Douda Naval Weapons Support Center Code 50C Crane, Indiana 47522-5050	1
Naval Civil Engineering Laboratory Attn: Dr. R. W. Drisko, Code L52 Port Hueneme, California 93401	1
Defense Technical Information Center Building 5, Cameron Station Alexandria, Virginia 22314	12 high quality
DTNSRDC Attn: Dr. H. Singerman Applied Chemistry Division Annapolis, Maryland 21401	1
Dr. William Tolles Superintendent Chemistry Division, Code 6100 Naval Research Laboratory Washington, D.C. 20375-5000	1
Dr. David Young Code 334 NORDA NSTL, Mississippi 39529	1
Naval Weapons Center Attn: Dr. Ron Atkins Chemistry Division China Lake, California 93555	1
Scientific Advisor Commandant of the Marine Corps Code RD-1 Washington, D.C. 20380	1
U.S. Army Research Office Attn: CRD-AA-IP P.O. Box 12211 Research Triangle Park, NC 27709	1
Mr. John Boyle Materials Branch Naval Ship Engineering Center Philadelphia, Pennsylvania 19112	1
Naval Ocean Systems Center Attn: Dr. S. Yamamoto Marine Sciences Division San Diego, California 91232	1

DL/1113/87/2

ABSTRACTS DISTRIBUTION LIST, SDIO/IST

Dr. Robert A. Osteryoung
Department of Chemistry
State University of New York
Buffalo, NY 14214

Dr. Douglas N. Bennion
Department of Chemical Engineering
Brigham Young University
Provo, UT 84602

Dr. Stanley Pons
Department of Chemistry
University of Utah
Salt Lake City, UT 84112

Dr. H. V. Venkatasetty
Honeywell, Inc.
10701 Lyndale Avenue South
Bloomington, MN 55420

Dr. J. Foos
EIC Labs Inc.
111 Downey St.
Norwood, MA 02062

Dr. Neill Weber
Ceramatec, Inc.
163 West 1700 South
Salt Lake City, UT 84115

Dr. Subhash C. Narang
SRI International
333 Ravenswood Ave.
Menlo Park, CA 94025

Dr. J. Paul Pemsler
Castle Technology Corporation
52 Dragon Ct.
Woburn, MA 01801

Dr. R. David Rauh
EIC Laboratory Inc.
111 Downey Street
Norwood, MA 02062

Dr. Joseph S. Foos
EIC Laboratories, Inc.
111 Downey Street
Norwood, Massachusetts 02062

Dr. Donald M. Schleich
Department of Chemistry
Polytechnic Institute of New York
333 Jay Street
Brooklyn, New York 01

Dr. Stan Szpak
Code 633
Naval Ocean Systems Center
San Diego, CA 92152-5000

Dr. George Blomgren
Battery Products Division
Union Carbide Corporation
25225 Detroit Rd.
Westlake, OH 44145

Dr. Ernest Yeager
Case Center for Electrochemical
Science
Case Western Reserve University
Cleveland, OH 44106

Dr. Mel Miles
Code 3852
Naval Weapons Center
China Lake, CA 93555

Dr. Ashok V. Joshi
Ceramatec, Inc.
2425 South 900 West
Salt Lake City, Utah 84119

Dr. W. Anderson
Department of Electrical &
Computer Engineering
SUNY - Buffalo
Amherst, Massachusetts 14260

Dr. M. L. Gopikanth
Chemtech Systems, Inc.
P.O. Box 1067
Burlington, MA 01803

Dr. H. F. Gibbard
Power Conversion, Inc.
495 Boulevard
Elmwood Park, New Jersey 07407

DL/1113/87/2

ABSTRACTS DISTRIBUTION LIST, SDIO/IST

Dr. V. R. Koch
Covalent Associates
52 Dragon Court
Woburn, MA 01801

Dr. Randall B. Olsen
Chronos Research Laboratories, Inc.
4186 Sorrento Valley Blvd.
Suite H
San Diego, CA 92121

Dr. Alan Hooper
Applied Electrochemistry Centre
Harwell Laboratory
Oxfordshire, OX11 ORA UK

Dr. John S. Wilkes
Department of the Air Force
The Frank J. Seiler Research Lab.
United States Air Force Academy
Colorado Springs, CO 80840-6528

Dr. Gary Bullard
Pinnacle Research Institute, Inc.
10432 N. Tantan Avenue
Cupertino, CA 95014

Dr. J. O'M. Bockris
Ementech, Inc.
Route 5, Box 946
College Station, TX 77840

Dr. Michael Binder
Electrochemical Research Branch
Power Sources Division
U.S. Army Laboratory Command
Fort Monmouth, New Jersey 07703-5000

Professor Martin Fleischmann
Department of Chemistry
University of Southampton
Southampton, Hants, SO9 5NH UK